ACS OMEGA

http://pubs.acs.org/journal/acsodf

Article

Synthesis of a Lignin-Enhanced Graphene Aerogel for Lipase Immobilization

Hong Zhang,* Xin Zhang, Lei Wang, Bo Wang, Xu Zeng, Bo Ren,* and Xiaodong Yang*

Cite This: *ACS Omega* 2023, 8, 2435−2444

Read Online

ACCESS | Metrics & More | Article Recommendations

ABSTRACT: A novel lignin-enhanced graphene aerogel (LGA) was prepared by one-step hydrothermal synthesis, and lipase from *Pseudomonas* sp. (PSL) was immobilized on LGA successfully by interfacial activation. The catalytic activity and enantioselectivity of LGA-PSL for the preparation of (*S*)-2-octanol by an enantioselective transesterification were improved obviously. The characterization of LGA and LGA-PSL was performed. X-ray diffraction and Fourier transform infrared spectroscopy demonstrated the formation of numerous electrostatic and hydrogen bonds between lignin and graphene in the aerogel structure. In addition, the specific surface area pore size analyzer (BET) test proved that the introduction of lignin significantly increased the specific surface area and pore size of the aerogel material, which improved the immobilization efficiency of lipase in the aerogel. The introduction of lignin has changed the original lamellar structure of the graphene oxide (GO) aerogels. The lignin cross-linked with the GO lamellae through hydrogen bonding, causing a porous structure to form between the original lamellae, thus increasing their specific surface area. The immobilized lipase (LGA-PSL) was used for the preparation of (*S*)-2-octanol by an enantioselective transesterification, and the reaction conditions for this enzymatic transesterification had been optimized. LGA-PSL exhibited a high catalytic performance and could be reused four times in this reaction. Based on these results, LGA as an immobilization carrier had potential applications in the industrial application of lipase.

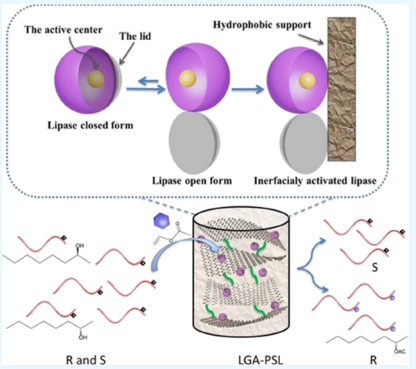

1. INTRODUCTION

Enzyme immobilization, defined as confining one or more enzymes in a defined space, was originally developed to solve the problems of enzyme recovery and reuse, during the middle of the previous century.[1,2] For the practical industrialization of enzymes, the strategies of enzyme immobilization have been widely studied to enhance the enzyme properties, such as regio- or enantio-selectivity, thermal stability, tolerance to organic solvents, and broad pH range.[3,4] The methods used for immobilization are varied in complexity and efficiency, such as physical adsorption, covalent attachment, physical entrapment, etc.[5−7] Among the immobilization techniques, stabilization needs to be properly designed, and the stabilization may be a consequence of different causes. The physical adsorption can be defined as one of the straightforward methods of reversible immobilization that has a higher capability of enzyme loading than other immobilization methods.[8] Adsorption can occur through weak nonspecific forces such as van der Waals force, ionic and hydrogen bonding, and hydrophobic interactions. Enzymes can be adsorbed on the surface of support carriers or in the pores of mesoporous materials, and the nature and morphology of the supports can influence the enzyme activity and stability obviously.[9−11]

Lipases (triacylglycerol acyl hydrolases, EC 3.1.1.3) are the most widely employed biocatalysts in organic synthesis.[12] In particular, lipase resolves the racemic substrate by a simple kinetic resolution to obtain chiral secondary alcohols and amines.[13] Massive studies have proven that the immobilization of lipases on hydrophobic supports could stabilize and activate, or even to improve enantioselectivity of the lipases.[14−17] Generally, most of the lipases cover the active site with a short α-helix called 'lid' or 'flap'.[18] In the presence of an interface, the lid is open and forms a hydrophobic channel together with the relevant parts. The substrate molecule can easily access the active site through a hydrophobic channel in the enzyme molecule, and the hydrophobic group of the lid forms a large hydrophobic space together with the hydrophobic region where the active site is located, acting as a large bioreactor and participating together in the catalysis of lipase.[19] When lipase is immobilized on the hydrophobic supports, the active center becomes exposed to the reaction medium, displacing the equilibrium to the open and active form. Therefore, immobilization of lipase on hydrophobic supports may become a tool to fix this open form of lipase.[20]

Received: October 26, 2022
Accepted: December 19, 2022
Published: January 4, 2023

https://doi.org/10.1021/acsomega.2c06908
ACS Omega 2023, 8, 2435−2444

Scheme 1. Schematic Illustration of the Preparation of the Lignin/Graphene Oxide Composite Aerogel (LGA) for Lipase Immobilization

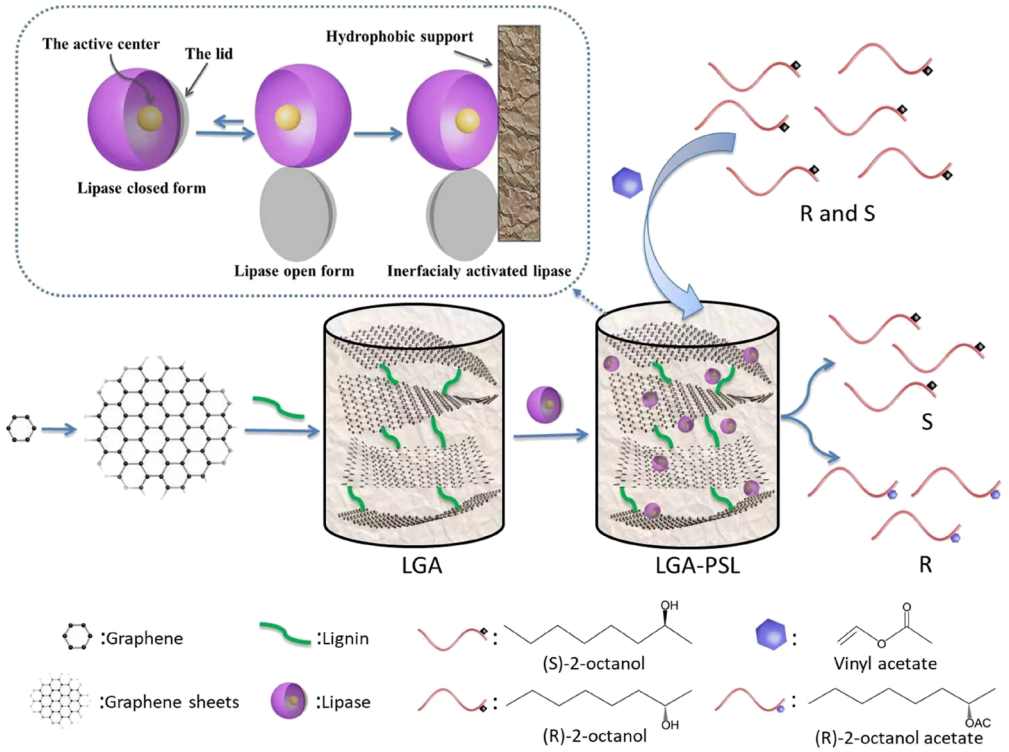

Graphene oxide (GO) has many excellent properties, such as large mechanical strength, a large specific surface area, high chemical stability, and good biocompatibility. Various oxygen-containing functional groups such as −COOH, −OH, C═O, and epoxide on its surface may become the key backbone for enzyme immobilization.[21] Furthermore, the hydrophobicity of GO is controlled by adjusting its degree of chemical reduction, and the increase in hydrophobic surface leads to an increase in lipase activity.[22] Zhang et al. reported the functionalization of GO with 3-mercaptopropyl trimethoxysilane. Though the immobilized lipase showed good pH, thermal stability, and storage stability, the nanoscale GO is difficult to recover from the catalytic reaction system.[23] Xie et al. prepared GO-Fe_3O_4 magnetic nanocomposites to develop a magnetically recoverable immobilized lipase.[24] However, magnetic nanocomposites tend to aggregate in catalytic reactions. The graphene aerogel has a three-dimensional porous network structure with high thermal stability, a large specific surface area, and high porosity.[25] It can not only effectively solve the aggregation behavior of graphene lamellae during the adsorption process, but also facilitate the mass transfer of the substrate and product during the reaction, thus improving the catalytic efficiency.[26,27] The large volume and low density of the aerogel material easily separate it from the reaction system and improve the recovery of the enzyme. Moreover, it has high mechanical strength, which enhances the stability of immobilized enzyme.[28] However, the structure of GO aerogels is unstable and prone to shrinkage and collapse.

Lignin is the only natural polymer containing an aromatic ring in nature. It is a three-dimensional network of polyphenolic polymeric aromatic compounds made of phenyl propane units connected by ether and carbon−carbon bonds.[29] Lignin has already been interesting to develop various applications according to its intrinsic properties, for instance, eco-friendliness, low toxicity, biocompatibility, lipophilicity, and susceptibility to degradation of enzymes.[24] In addition, it was reported that the aromatic biopolymer lignin consisted of a hydrophobic phenyl propane skeleton and oxygen-containing branches, which can link with GO sheets via hydrogen bonding, $\pi-\pi$ conjugation and van der Waals force.[30] Thus, lignin displays great possibility to modify the graphene aerogel. Lignin was introduced as a modifier to enhance the stability of graphene aerogels.[31,32] At the same time, the introduction of lignin also significantly increases the specific surface area and pore size of the aerogel material, which improves the immobilization efficiency of lipase in the aerogel, thereby increasing the stability and catalytic efficiency of the enzyme.[33,34]

In this work, we investigate the preparation of a lignin-based graphene oxide-reinforced composite aerogel with a three-dimensional mesh-like porous structure by a simple and environmentally friendly method. This aerogel material was used for the immobilization of lipase (PSL). The morphology and sample appearance of the materials were characterized by scanning electron microscopy (SEM), specific surface area pore size analyzer (BET), X-ray diffraction (XRD), and Fourier transform infrared (FT-IR) spectroscopy, respectively. Then we used the enhanced aerogel material to study the immobilization of lipase. The lipase was introduced into this aerogel by adsorption. The immobilized lipase (PSL-LGA) was used for the resolution of racemic 2-octanol via an enantioselective transesterification, and the reaction conditions for this enzymatic transesterification have been optimized. The full kinetic process of the ester exchange catalytic reaction consists of the following steps. The molecules of the reactants diffuse toward the active center of the resin catalyst, the reactants undergo adsorption, reaction and product desorption

https://doi.org/10.1021/acsomega.2c06908
ACS Omega 2023, 8, 2435−2444

on the catalyst surface, and the products diffuse from the active center of the catalyst to the main body of the liquid phase.[35]

As shown in Scheme 1, there was a flexible and relatively conserved region in the lipase: the "lid". The active center of lipase was hidden inside this "lid". During the process of aerogel immobilization of lipase, the hydrophobic interface of the aerogel could effectively activate the conformational change of lipase. This hydrophobic interface interacted with the hydrophobicity surrounding the active center of the lipase, causing the lipase's "lid" to open (active) or closed (inactive). That is to say, the hydrophobic interface of the aerogel makes the "lid" of the lipase easier to open, and it is easier to expose the active center, thereby improving the catalytic activity and stability of the enzyme. Using the lignin-enhanced graphene aerogel material as the carrier of the immobilized enzyme not only improves the structural stability of the aerogel, but also improves the use efficiency of the immobilized enzyme and the stability of the enzyme. It will have potential application value in the industrial application of lipase.

2. MATERIALS AND METHODS

2.1. Materials. GO (5 mg/mL), high-purity flake graphite, vinyl acetate, 2-octanol, hexane, and other analytical reagents were purchased from J&K Scientific Co., Ltd.. Lignin was purchased from Aladdin Reagent (Shanghai) Co., Ltd. Lipase from *Pseudomonas* sp. (PSL) and *R*-(+)-1-Phenylethyl isocyanate (*R*-(+)-PELC) were purchased from Tokyo Chemical Industry (TCI) Co., Ltd. All reagents were used as received without further purification. Experimental instruments, PerkinElmer FT-IR Spectrometer Spectrum Two, powder XRD, a MicrotracBEL BELSORP MINI II surface area/pore size distribution analyzer, Rigaku SmartLabSE, Lyovapor L-200 Pro, himac centrifuge CF16RN, HZQ-X100 shaking incubator, TWCl-B temperature-regulating magnetic stirrer, and JC-101 electric heating blast drying oven, were used.

2.2. Synthesis of LGA. Ten milliliters of GO was dissolved in 10 mL of 60% alcohol to form a homogeneous solution. A certain amount of lignin and GO alcohol solution was mixed with a vortex shaker (3000 rpm) for 1 min and then sonicated for 10 min to obtain a stable suspension. The mixture was sealed in a 25 mL Teflon-lined autoclave and heated at 180 °C for 12 h. After the autoclave was cooled to room temperature, the as-obtained hydrogel was washed with deionized water several times and then freeze-dried at −60 °C for 12 h to get LGA. The pure graphene aerogel (GA) was also obtained according to a similar procedure.

2.3. Lipase Immobilized on LGA. Ten grams of enzyme powder was added to 1 L of deionized water, stirred at 4 °C for 2 h, and centrifuged at 8000 rpm. The insoluble matter in water is removed, and the enzyme solution is lyophilized to obtain a preliminary purified enzyme powder. One gram of lyophilized enzyme powder was dissolved in 100 mL, pH 7.0 phosphate buffer (10 mM) to make 10 mg/mL of enzyme solution.

A whole piece of the above synthesized LGA is taken and cut into uniform (5 × 15) mm pieces. 0.1 g of the above cut LGA adsorbent was immersed in 10.0 mL of the above-prepared enzyme solution. The immobilized enzyme was stirred for 4 h at room temperature, and the resulting immobilized enzyme was filtered and washed three more times with deionized water. The immobilized PSL was dried overnight under vacuum. The amount of PSL immobilized on the support (260 mg/g) was measured by the Lowry method with BSA as a standard for protein concentration.[36]

2.4. Resolution of (*R*,*S*)-2-Octanol Catalyzed by Lipase. The reaction was performed in a round bottom flask containing (*R*,*S*)-2-octanol (1 mmol), vinyl acetate (4 mmol), *n*-hexane (10 mL), water activity (a_w = 0.40), PSL (10.3 mg), or immobilized PSL (50 mg) that had the same protein content at 50 °C for 12 h. One unit of enzymatic activity (U) is defined as the amount of enzyme required to produce 1 μmol of 2-octanol acetate per min in the first 0.5 h (Scheme 2). The immobilized PSL was recovered by centrifugation (3000 rpm, 15 min) after each batch and was reused for the next batch reaction under the same conditions.

Scheme 2. Resolution of 2-Octanol Catalyzed by the Immobilized PSL

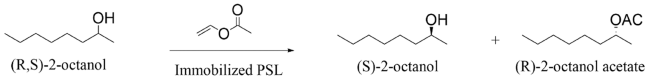

2.5. Determination of Enantiomeric Excess Values and Enantioselectivity. The samples were withdrawn from the vials and analyzed directly by a gas chromatograph on a Shimadzu gas chromatograph (GC-14B) equipped with an FID detector and a column (EC-1000, 30 m × 0.25 mm × 0.25 μm, Alltech). The temperatures of the injector and the detector were 200 and 290 °C, respectively. Nitrogen was used as the carrier gas at a flow rate of 60 mL/min. Temperature programming between 110 and 210 °C with the increment of 15 °C/min was used to determine the concentration of 2-octanol. (*S*)-2-Octanol or (*R*)-2-octanol was derived from *R*-(+)-PELC (Scheme 3). The distinction of *R* from *S*

Scheme 3. Formation of Isomers for Precolumn Derivation

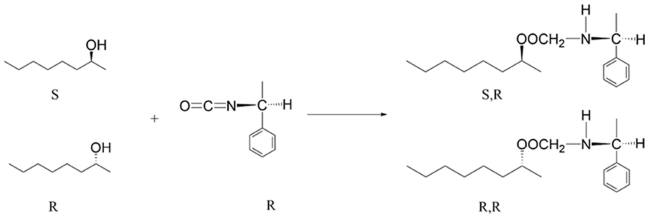

enantiomers was achieved with temperature programming between 110 and 222 °C with an increment of 10 °C/min. The retention time for *S* and *R* diastereomer was 12.36 and 12.84 min, respectively.

The degree of conversion (*C*) was determined from the ratio of the peak areas of the produced 2-octanol acetate to the total peak areas of the residuary 2-octanol and the produced 2-octanol acetate. The enantiomeric excess (ee_S) of the 2-octanol was determined by calculating the peak areas of the two derivatives. The enantiomeric ratio (*E* value) was determined from *C* and ee_S by using eq 1:[36]

$$\text{enantiomeric excesses, } ee_S\ (\%) = \frac{[S-R]}{[S+R]} \times 100$$

$$\text{enantioselectivity, } E = \frac{\ln[(1-C)(1-ee_s)]}{\ln[(1-C)(1+ee_s)]} \quad (1)$$

where *S* and *R* represent the concentrations of the (*S*,*R*)-diastereomer and (*R*,*R*)-diastereomer, respectively.

https://doi.org/10.1021/acsomega.2c06908
ACS Omega 2023, 8, 2435−2444

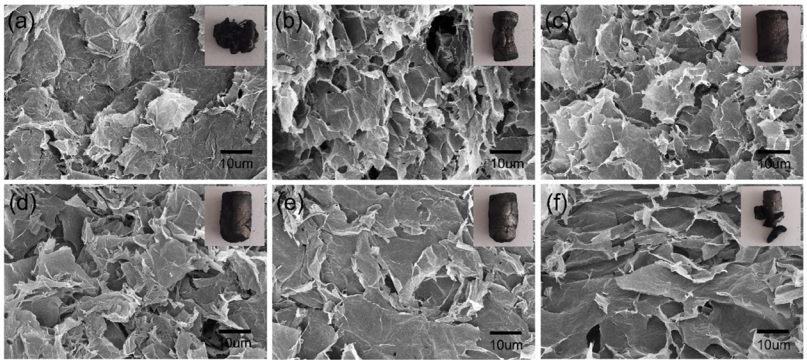

Figure 1. SEM photographs of the surface and cross section of GA (a), LGA-0.2 (b), LGA-0.4 (c), LGA-0.6 (d), LGA-0.8 (e), and LGA-1 (f), respectively.

3. RESULTS AND DISCUSSION

3.1. Characterization of the LGA Composite Aerogel.

3.1.1. SEM Characterization. As can be seen from the SEM images, the lignin and GO composite aerogel materials (LGAs) formed a 3D network porous structure. Figure 1a showed that when the ratio of lignin to GO was 0:1, only GO existed in the aerogel material, forming a large layered structure, and the collapse of the aerogel structure could be seen macroscopically. When the ratio of lignin to GO was 0.2:1, an aerogel with a smaller lamellar structure was formed. As shown in Figure 1b, the introduction of lignin made the structure of the aerogel shrink. When the lignin content increased to 0.4:1, a more uniform layered network structure was formed. As shown in Figure 1c, these layers were all about 10 μm. Macroscopically, the aerogel kept a regular shape. This was essential for the immobilization of lipase. When the ratio of lignin to GO reached 0.6:1, the structure became slightly larger. As shown in Figure 1d, the aerogel showed a loose structure and tended to swell. When the ratio of lignin to GO reached 0.8:1, the lamellar in the structure continued to increase in size and the pore size became smaller. As shown in Figure 1e, the corresponding aerogel structure had slightly deformed. When the ratio of lignin to GO reached 1:1, a large layer structure was formed in the structure. These lamellar structures were almost joined together in sheets, probably due to the excessive lignin content, which caused the aerogel pore size to disappear. The aerogel as shown in Figure 1f had difficulty in maintaining a certain structure, and macroscopic fragmentation of the aerogel could be seen. In summary, we found an optimum ratio of 0.4:1 of lignin to GO for the formation of aerogels. The LGA used in the subsequent immobilization experiments was also prepared in this ratio. The appropriate ratio made the pore structure stable and homogeneous, which facilitated the entry of lipase and increased the adsorption efficiency.

3.1.2. X-ray Diffractometer. In order to compare the structural changes of this series of aerogel materials, we carried out XRD tests. As shown in Figure 2, GO had a relatively sharp characteristic diffraction peak around 10.3°. Compared with GO, the peaks of GA, LGA-0.2, LGA-0.4, LGA-0.6, LGA-0.8, and LGA-1 exhibit relatively broad low diffraction angles (2θ = 24.9°), in which there were no relatively sharp characteristic diffraction peaks around 10.3°. This was due to the reduction of GO during the hydrothermal synthesis to prepare the aerogel, resulting in the removal of oxygen in the interlayer of graphene oxide. As a result, the spacing between the graphene layers became smaller, and the structure changes significantly, resulting in a shift of the diffraction angle around 10.3° and a

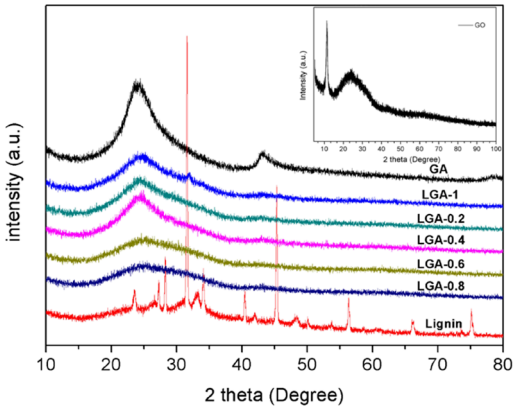

Figure 2. XRD of GA aerogel, LGA aerogel, GO, and lignin.

wider peak shape. With the increase of the amount of lignin added, the intensity of the characteristic diffraction peak at 24.9° became weaker and the peak shape became wider. It showed that the electrostatic and hydrogen bonds between the lignin and graphene sheets had been generated, resulting in the influence of the structure. However, the interlayer spacing of the LGA was calculated to be 3.60 Å from the characteristic peak at 2θ = 24.9°, which was similar to that of GA.[32] It showed that during the formation of the aerogel, GO and lignin bond together into a noncrystalline structure, and therefore, the lignin peak disappeared, which was consistent with the XRD data. The increase in disordered parts and lattice defects on the surface of the LGA and the decrease in the ordered lattice made the original diffraction peaks of lignin weaker or even disappear. This showed that the lignin-modified graphene aerogel could well maintain the overall structure of the GA even if electrostatic and hydrogen bonds were generated between the lignin and graphene. It also showed that the addition of lignin effectively enhanced the mechanical strength of GAs. That is, the introduction of lignin molecules into GA had little effect on the ordered layered structure, but could enhance the overall mechanical strength of GA. In addition, the reduction of GO endowed the series of lignin-modified aerogel materials with a hydrophobic interface. The hydrophobic interface of the aerogel could effectively activate the conformational change of the lipase, making the "lid" of the lipase easier to open and expose the active center, thereby improving the catalytic activity and stability of the enzyme.

https://doi.org/10.1021/acsomega.2c06908
ACS Omega 2023, 8, 2435−2444

3.1.3. FT-IR Test. To demonstrate how lignin interacted with graphene, we performed FT-IR spectroscopy on LGA series samples. As shown in Figure 3, lignin showed a strong C=C

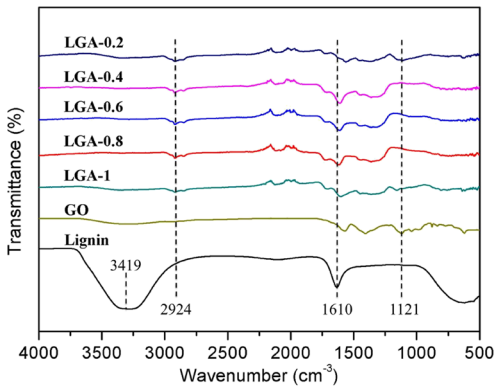

Figure 3. FT-IR spectra of the GA aerogel, LGA aerogel, GO, and lignin.

bond stretching vibration peak at 1610 cm^{-1}, while the GA showed a relatively weak vibration peak. After the introduction of lignin into GO, the peaks at 1610 cm^{-1} in the LGA system were enhanced compared to GA, indicating that there was an interaction between lignin and graphene. The aliphatic carbon chain peak of lignin appeared in the LGA at 2924 cm^{-1}, indicating that the lignin and GO were cross-linked together by hydrogen bonding interaction. The −OH stretching vibration peak of lignin at 3419 cm^{-1} and the C−O−C stretching vibration peak of GO at 1121 cm^{-1} both disappear in the LGA.[31] It showed that the −OH of the lignin and the C−O−C of the GO were reduced during the formation of aerogel, which was consistent with the XRD data. In conclusion, the LGA aerogel maintained the structure of GO, that is, the introduction of lignin did not change the overall structure of the aerogel. It was only through hydrogen bonding that the lignin and GO were cross-linked, which made the aerogel structure more compact and the mechanical properties more stable.

3.1.4. Specific Surface Area Method (BET). The specific surface area and pore structure of GA and LGAs were measured by an automated surface area and pore size distribution analyzer using the Brunauer−Emmett−Teller (BET) technique. Table 1 summarized the surface area, cumulative pore volume, and average pore size width of LGA composite aerogels and GA. All aerogels could be classified as ultralight materials because their density was less than 10 mg/cm^3. It could be seen from Table 1 that LGA-0.4 had the largest specific surface area, which was 114 m^2/g, which was much larger than that of other materials. Compared with GA of 0.1014 cm^3/g and 8.4856 nm, LGA-0.4 had the largest pore volume of 0.3367 cm^3/g and an average pore size of 11.854 nm. Obviously, all the isotherms were type IV isotherms with H3-type hysteresis loops as shown in Figure 4a−f, indicating typical mesoporosity.[37] This enlarged surface area, porous structure of LGA was related to the effect of lignin on the pore structure. The pore size of the carrier material had a great influence on the adsorption of the enzyme, and the appropriate pore size could improve the enzyme loading and the activity of the immobilized enzyme. In addition, within a certain range, with the increase of lignin content, the specific surface area, pore volume, and pore size of aerogel beads increased, which was beneficial to the mass transfer of the substrate and its products during the reaction process, thereby improving the adsorption efficiency. Compared with GA, the LGA composite aerogel had a larger pore volume and specific surface area, which was consistent with the above SEM analysis results.

Table 1. Physical Properties of the GA Aerogel and LGA Aerogel

sample	density (mg/cm^3)	BET surface area (m^2/g)	cumulative volume of pores (cm^3/g)	pore average width (nm)
GA	8.2	47.8	0.1014	8.4856
LGA-0.2	5.6	52.3	0.2349	17.952
LGA-0.4	3.4	114	0.3367	11.854
LGA-0.6	4.0	74.1	0.186	10.036
LGA-0.8	6.1	53.6	0.1154	8.6052
LGA-1	5.8	65.1	0.1686	10.366

3.2. Immobilization and Stabilities. *3.2.1. Immobilization of PSL.* To confirm whether PSL was successfully immobilized on LGA-0.4, the FT-IR spectra of LGA-0.4, PSL, and immobilized PSL were studied. As shown in Figure 5, the strong absorption band at 3273 cm^{-1} indicated that PSL had a large number of N−H groups. After being immobilized by the LGA composite aerogel material, the N−H groups formed hydrogen bonds with the hydrogen in the lignin, and the intensity band of this absorption was drastically reduced. Furthermore, relatively strong C−O stretching (about 1631 cm^{-1}) and C−H deformation (about 1515 cm^{-1}) related absorption bands can be observed in the PSL and LGA-PSL spectra. However, these two absorption bands were not observed in the LGA-0.4 spectrum. These results confirm that PSL had been successfully immobilized on the LGA.

3.2.2. Comparison of the Catalytic Properties of Immobilized PSL with that of Free PSL. Free lipase and lipase immobilized onLGA-0.4 were used to solve for resolution of (*R*,*S*)-2 octanol. As shown in Table 2, it was found that the activity and enantioselectivity of the lipase were improved by immobilization on LGA-0.4.

It is well known that a promising property of lipase is its interfacial activation in the presence of a hydrophobic interface, which was reported by Sarada and Desnuelle.[38] There was a flexible and relatively conserved region in the lipase: the "lid". The active center of lipase was hidden inside this "lid". During the process of aerogel immobilization of lipase, the hydrophobic interface of the aerogel could effectively activate the conformational change of lipase. This hydrophobic interface interacted with the hydrophobicity surrounding the active center of the lipase, causing the lipase's "lid" to open (active) or closed (inactive). That is to say, the hydrophobic interface of the aerogel makes the "lid" of the lipase easier to open, and it is easier to expose the active center, thereby improving the catalytic activity and stability of the enzyme. When some other hydrophobic surfaces of the protein chains are strongly adsorbed onto the hydrophobic support, a dramatic change in the enzyme conformation may occur, which may alter the enantioselectivity of the lipase.

3.2.3. Effect of Temperature. The effect of temperature on the activity and enantioselectivity of immobilized PSL in resolution of 2-octanol was investigated at various temperatures. As shown in Figure 6, the activity of the immobilized enzyme increased as the reaction temperature increased from 30 to 55 °C. A maximum enzymatic activity of 480 μmol/g·min was observed at 55 °C, but the enzymatic activity

https://doi.org/10.1021/acsomega.2c06908
ACS Omega 2023, 8, 2435−2444

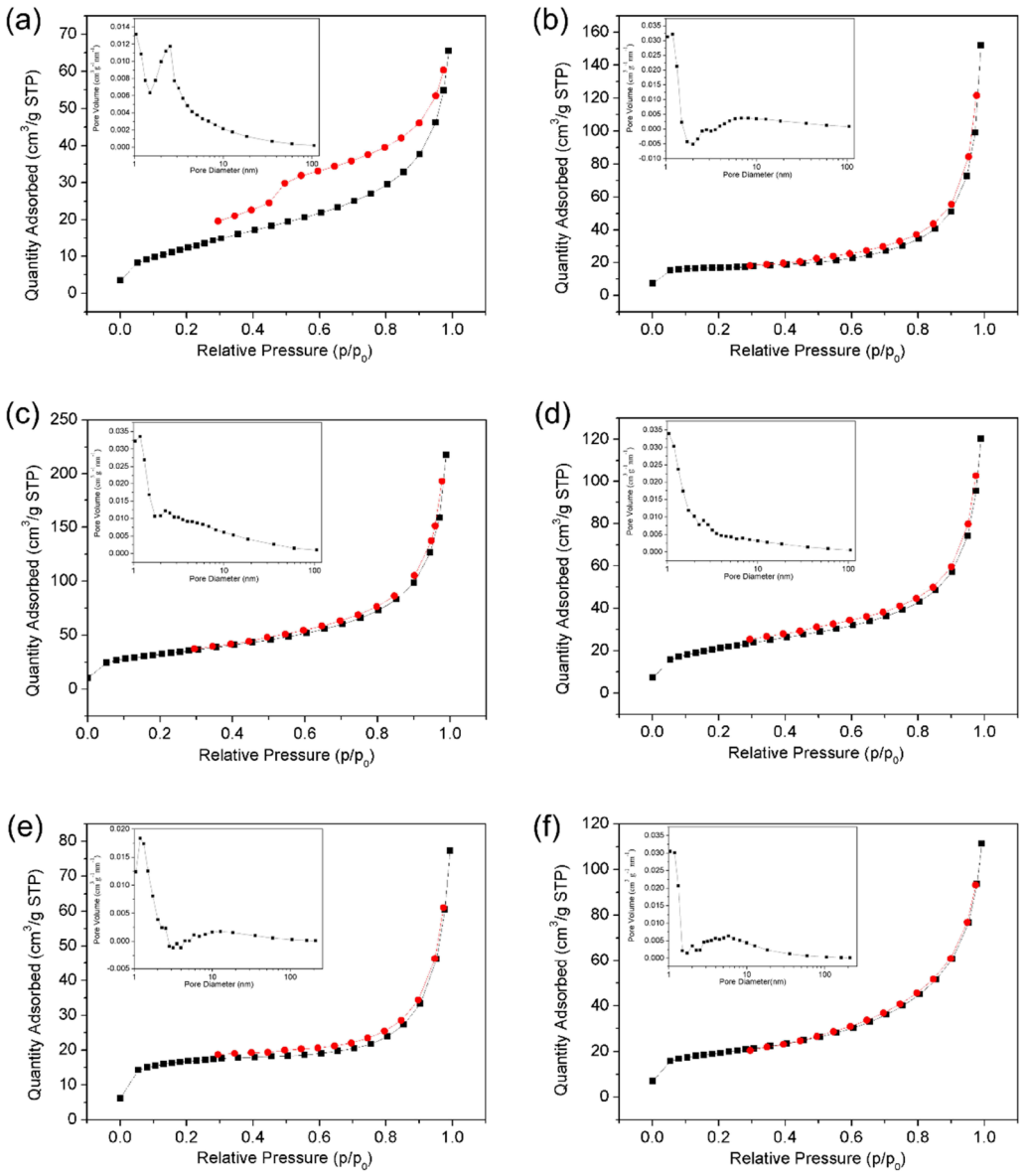

Figure 4. Surface area of GA aerogel and LGAs aerogel. GA (a), LGA-0.2 (b), LGA-0.4 (c), LGA-0.6 (d), LGA-0.8 (e), and LGA-1 (f).

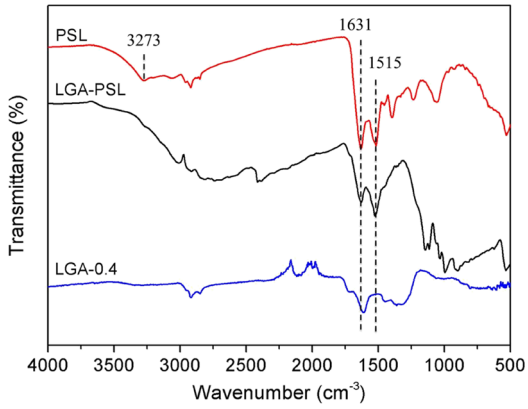

Figure 5. FT-IR spectra of PSL, LGA-0.4, and PSL-LGA.

decreased sharply from 55 to 65 °C. As the reaction temperature increases, the chance of the enzyme colliding with the substrate molecules increases, which may help to form enzyme-substrate complexes and then improve the reaction rate. In addition, the enhanced protein fluctuation caused by higher temperature can alleviate the steric repulsion between the enzyme and the substrate, which also has the potential to speed up the reaction rate.[39] With further increase in temperature, the interaction between noncovalent bonds may be disrupted by heat-induced effects, so the spatial conformation of the enzyme is disrupted,[40] resulting in a decrease in enzyme activity. The enantioselectivity (E value) decreased with the increase of the reaction temperature, which

Table 2. Comparison of the Catalytic Properties of Free and Immobilized PSL under Optimum Reaction Conditions[a]

samples	bound protein (mg/g)	activity (μmol/g·min)	E value
free PSL		124.6	49
LGA-0.4-PSL	260	480	97

[a]Reactions were carried out in n-hexane (10 mL) with (R,S)-2-octanol (1 mmol), vinyl acetate (4 mmol), and free (10.3 mg) or immobilized PSL (50 mg) that had the same protein content and water activity (a_w) of 0.40 at 55 °C for 12 h.

https://doi.org/10.1021/acsomega.2c06908
ACS Omega 2023, 8, 2435−2444

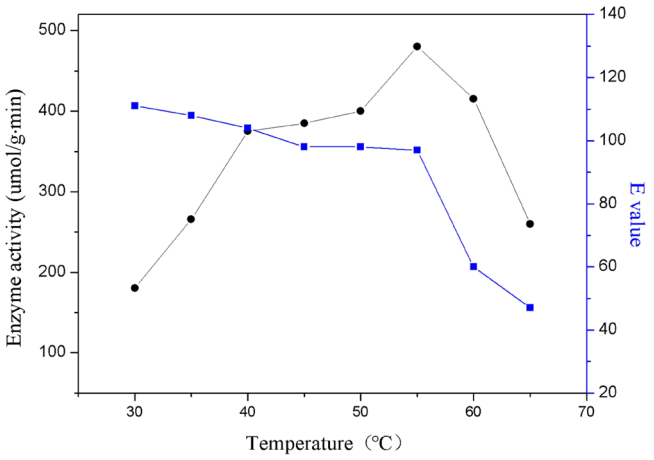

Figure 6. Effect of temperature on the activity (solid circle) and enantioselectivity (solid box) of immobilized PSL in transesterification. Reactions were carried out in *n*-hexane (10 mL) with (*R*,*S*)-2-octanol (1 mmol), vinyl acetate (4 mmol), immobilized PSL (50 mg), and a_w (0.40) at different temperatures (30−65 °C) for 12 h.

was consistent with the results of Phillips, who found that the enzyme exhibited the best enantioselectivity at low temperature.[41] In general, the enzyme activity was highest at 55 °C while maintaining a high *E* value (97). Therefore, 55 °C was chosen as the optimal temperature for this reaction.

3.2.4. Water Activity. Water may play an important role for the enzyme to maintain its proper conformation to maintain its catalytic activity when the enzyme is used in a non-aqueous medium. In recent years, the amount of water available to enzymes in non-aqueous reaction systems is often quantified by thermodynamic water activity (a_w),[42] which can be controlled by adding salts or salt hydrates to organic solvents or substrates, as reported by Haring.[43] In this study, the reactions catalyzed by immobilized PSL were carried out from the a_w value of 0.05 to 0.95, and the results are shown in Figure 7. We observed a bell-shaped curve of enzyme activity as a function of water activity in Figure 7. At low a_w values (0.05−0.40), lower enzyme activity was observed. When a_w = 0.40, the immobilized enzyme LGA-0.4-PSL showed the highest

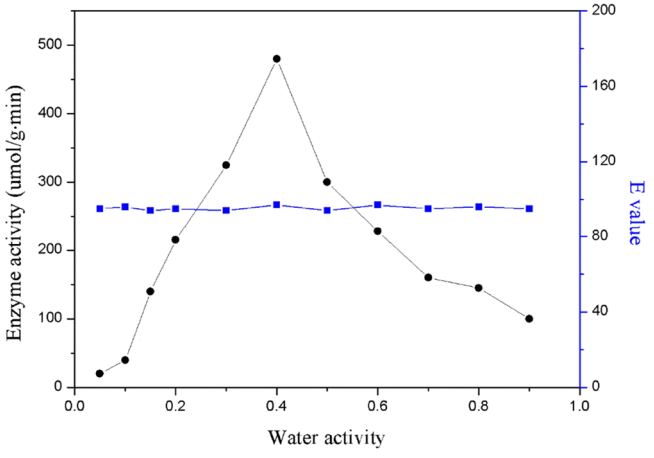

Figure 7. Effect of water activity on the activity (solid circle) and enantioselectivity (solid box) of immobilized PSL in transesterification. Reactions were carried out in *n*-hexane (10 mL) with (*R*,*S*)-2-octanol (1 mmol), vinyl acetate (4 mmol), immobilized PSL (50 mg), and a_w (0.05−0.95) at 55 °C for 12 h.

activity. However, increasing the a_w value from 0.40 to 0.95 resulted in a sharp drop on enzyme activity. Since the conformation of PSL is too rigid at low water activity, this may interfere with the "induced fit" process of PSL and reduce enzymatic activity,[44] while the decrease in enzyme activity at higher a_w values can be attributed to the observed aggregation of enzyme particles, which may in turn limit substrate access to the enzyme active site. Another explanation might be that the overly flexible conformation of enzyme molecule at a higher a_w value reduces transesterification activity. These results suggest that water activity strongly affects the hydration level of the enzyme, which in turn affects its transesterification activity. The results of this study show that the *E* value remains almost unchanged as the a_w value changes. A possible explanation is that water may not act as a competitive nucleophile for the acylase intermediate in this reaction, so the enantioselectivity is not affected by water activity.[45]

3.2.5. Substrate Ratio. As shown in Figure 8, the effect of molar ratios of vinyl acetate to 2-octanol from 1:1 to 7:1 on

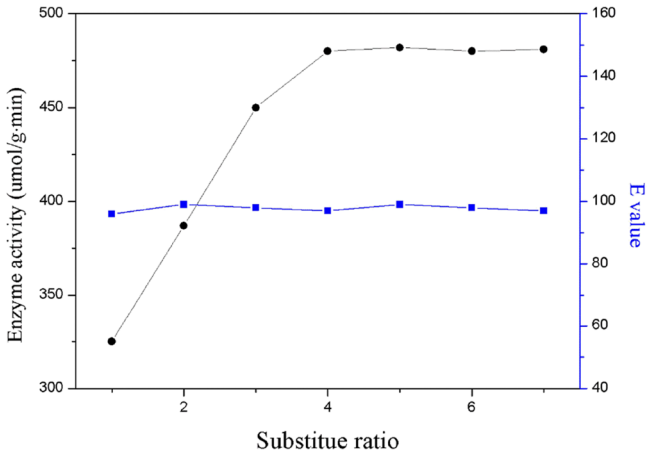

Figure 8. Effect of substrate ratio on the activity (solid circle) and enantioselectivity (solid square) of immobilized PSL in transesterification. Reactions were carried out in *n*-hexane (10 mL) with immobilized PSL (50 mg) and a_w (0.40) at 55 °C for 12 h. The concentration of 2-octanol was kept constant (1 mmol), whereas the concentration of vinyl acetate was varied from 1 to 7 mmol.

transesterification was investigated. We observed that when the amount of enzyme was kept constant, the substrate ratio continued to increase, and the enzyme activity gradually increased until the increase reached the maximum value. After this point (4:1), the enzymatic activity could not increase with increasing substrate ratio. On the other hand, enantioselectivity was not affected by increasing the ratio of substrates.

3.2.6. Effect of the Amount of Immobilized PSL. Different amounts of immobilized lipase (20−80 mg) were added to the reaction mixture, and it was found that the rate of the transesterification reaction increased as the amount of immobilized lipase increased. The enzyme activity reached a maximum when 50 mg of immobilized lipase was used (Figure 9). However, for amounts of lipase above 50 mg, the difference almost leveled off. The *E* value was not affected when changing the amount of immobilized PSL.

3.2.7. Reusability of Enzyme. In general, free enzymes are difficult to recover and reuse. The use of immobilized enzymes may help reduce product costs and make enzymatic processes economically viable.[45] Subsequent reusability studies were

https://doi.org/10.1021/acsomega.2c06908
ACS Omega 2023, 8, 2435−2444

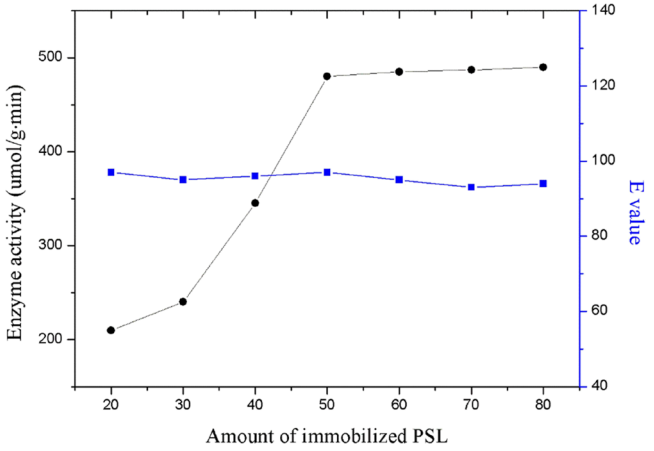

Figure 9. Effect of the amount on the activity (solid circle) and enantioselectivity (solid box) of immobilized PSL in transesterification. Reactions were carried out in *n*-hexane (10 mL) with (*R*,*S*)-2-octanol (1 mmol), vinyl acetate (4 mmol), a_w (0.40) at 55 °C for 12 h, whereas the amount of immobilized PSL was varied from 20 to 80 mg.

performed by using the recovered lipase. The results in Figure 10 show that the immobilized PSL retained 94% activity after

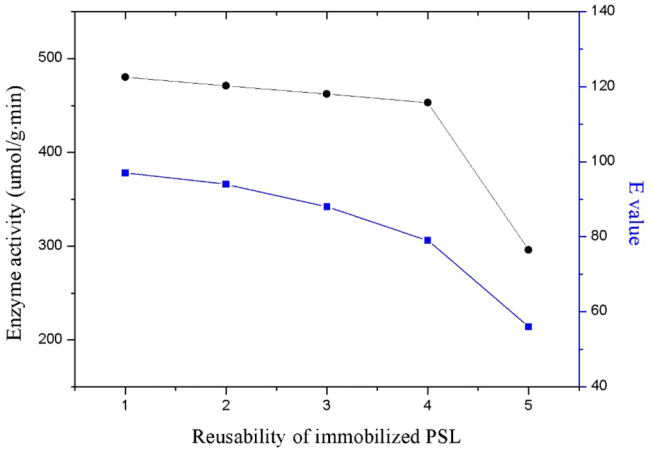

Figure 10. Activity (solid circle) and enantioselectivity (solid box) of immobilized PSL in repeated batch process by LGA-0.4-PSL. Reactions were carried out in *n*-hexane (10 mL) with (*R*,*S*)-2-octanol (1 mmol), vinyl acetate (4 mmol), immobilized PSL (50 mg), and a_w (0.40) at 55 °C for 12 h.

four cycles without significant change in the *E* value. However from the fifth cycle, the enzyme activity began to gradually decrease. The results show that the immobilized lipase has the possibility to be reused, but it is still not ideal because the activity of the immobilized lipase decreases during continuous reuse. This may be closely related to the leaching of PSL from the carrier to the free enzyme. The leaching of PSL may be due to the weak interaction between the PSL molecules and the surface of the hydrophobic support. Leakage of adsorbed enzymes into the reaction mixture is a common disadvantage of adsorption immobilization techniques. Another possibility is mechanical loss during filtration and drying of the immobilized enzymes.

4. CONCLUSIONS

We prepared a novel lignin-enhanced graphene aerogel (LGA) material by a one-step hydrothermal synthesis method. The aerogel material with enhanced mechanical strength had many advantages in enzyme immobilization; that is, it effectively maintains the stability of the enzyme, increases the catalytic efficiency, and brings convenience to the post-processing of the catalytic reaction. In the LGA, electrostatic and hydrogen bonds were formed between lignin and GO, which made the overall structure of the aerogel more stable. At the same time, the introduction of lignin significantly increased the specific surface area and pore size of the aerogel material, thereby improving the immobilization efficiency of lipase in the aerogel. XRD and FT-IR tests proved that many electrostatic and hydrogen bonds were formed between lignin and graphene in the aerogel structure, which made the structure of the aerogel more stable. It was more intuitively observed by SEM that the addition of lignin made the graphene aerogel structure more stable. In terms of applications, we performed immobilization studies of lipase using this novel enhanced aerogel material. The BET test proved that the introduction of lignin significantly increased the specific surface area and pore size of aerogel materials, improved the immobilization efficiency of lipase in aerogels, and improved the stability and catalytic efficiency of lipase. In the resolution of (*R*,*S*)-2-octanol, LGA-0.4-PSL exhibited not only the higher catalytic activity and enantioselectivity, but also satisfactory reusability. Under the optimum conditions, the residual 2-octanol was recovered with 99.5% enantiomeric excess at 52.9% conversion rate. The immobilized PSL also proved to be stable, with little loss of activity when it was used repeatedly. After four catalytic cycles of use, the activity of the immobilized lipase remained at over 94% of the initial activity. That was to say, the lipase immobilized by this new lignin-enhanced aerogel material greatly increases the stability of the enzyme and greatly improved the reusability of the lipase. In conclusion, using LGA as a carrier for immobilized enzymes not only improved the structural stability of aerogels, but also improved the catalytic efficiency and stability of the immobilized enzymes. It would have potential application value in the industrial application of lipase.

AUTHOR INFORMATION

Corresponding Authors

Hong Zhang − *Institute for Interdisciplinary Biomass Functional Materials Studies, Jilin Engineering Normal University, Changchun 130052, P.R. China*; orcid.org/0000-0002-8105-6422; Email: zhanghong19870825@126.com

Bo Ren − *Institute for Interdisciplinary Biomass Functional Materials Studies, Jilin Engineering Normal University, Changchun 130052, P.R. China*; Email: ren20121217@126.com

Xiaodong Yang − *Institute for Interdisciplinary Biomass Functional Materials Studies, Jilin Engineering Normal University, Changchun 130052, P.R. China*; Email: y86908051@126.com

Authors

Xin Zhang − *Institute for Interdisciplinary Biomass Functional Materials Studies, Jilin Engineering Normal University, Changchun 130052, P.R. China*

https://doi.org/10.1021/acsomega.2c06908
ACS Omega 2023, 8, 2435−2444

Lei Wang − *Key Laboratory of Molecular Enzymology and Engineering of Ministry of Education, Jilin University, Changchun 130023, P.R. China;* orcid.org/0000-0002-9728-0613

Bo Wang − *Institute for Interdisciplinary Biomass Functional Materials Studies, Jilin Engineering Normal University, Changchun 130052, P.R. China*

Xu Zeng − *Institute for Interdisciplinary Biomass Functional Materials Studies, Jilin Engineering Normal University, Changchun 130052, P.R. China*

Complete contact information is available at: https://pubs.acs.org/10.1021/acsomega.2c06908

Notes

The authors declare no competing financial interest.

■ ACKNOWLEDGMENTS

We acknowledge financial support from the Education Department of Jilin Province [JJKH20210170KJ, JJKH20210171KJ] and the Jilin Engineering Normal University Academic Research Project [No. BSKJ201904, No. BSKJ201837].

■ REFERENCES

(1) Bolivar, J. M.; Woodley, J. M.; Fernandez-Lafuente, R. Is enzyme immobilization a mature discipline? Some critical considerations to capitalize on the benefits of immobilization. *Chem. Soc. Rev.* **2022**, *51*, 6251−6290.

(2) Fernandez-Lafuente, R. Editorial for Special Issue: Enzyme Immobilization and Its Applications. *Molecules* **2019**, *24*, 4619−4623.

(3) Garcia-Galan, C.; Berenguer-Murcia, Á.; Fernandez-Lafuente, R.; Rodrigues, R. C. Potential of Different Enzyme Immobilization Strategies to Improve Enzyme Performance. *Adv. Synth. Catal.* **2011**, *353*, 2885−2904.

(4) Mateo, C.; Palomo, J. M.; Fernandez-Lorente, G.; Guisan, J. M.; Fernandez-Lafuente, R. Improvement of enzyme activity, stability and selectivity via immobilization techniques. *Enzyme Microb. Technol.* **2007**, *40*, 1451−1463.

(5) Mohamad, N. R.; Marzuki, N. H. C.; Buang, N. A.; Huyop, F.; Wahab, R. A. An overview of technologies for immobilization of enzymes and surface analysis techniques for immobilized enzymes. *Biotechnol. Biotechnol. Equip.* **2015**, *29*, 205−220.

(6) Miletić, N.; Nastasović, A.; Loos, K. Immobilization of biocatalysts for enzymatic polymerizations: Possibilities, advantages, applications. *Bioresour. Technol.* **2012**, *115*, 126−135.

(7) Cantone, S.; Ferrario, V.; Corici, L.; Ebert, C.; Fattor, D.; Spizzo, P.; Gardossi, L. Efficient immobilisation of industrial biocatalysts: criteria and constraints for the selection of organic polymeric carriers and immobilisation methods. *Chem. Soc. Rev.* **2013**, *42*, 6262−6276.

(8) Jesionowski, T.; Zdarta, J.; Krajewska, B. Enzyme immobilization by adsorption: a review. *Adsorption* **2014**, *20*, 801−821.

(9) Nguyena, H. H.; Kim, M. An Overview of Techniques in Enzyme Immobilization. *Appl. Sci. Converg. Technol.* **2017**, *26*, 157−163.

(10) Liu, X.-L.; Verma, G.; Chen, Z.-S.; Hu, B.-W.; Huang, Q.-F.; Yang, H.; Ma, S.-Q.; Wang, X.-K. Metal-organic framework nanocrystal-derived hollow porous materials: Synthetic strategies and emerging applications. *Innovation* **2022**, *3*, 100281−100297.

(11) Zhang, Y.-F.; Liu, H.-X.; Gao, F.-X.; Tan, X.-L.; Cai, Y.-W.; Hu, B.-W.; Huang, Q.-F.; Fang, M.; Wang, X.-K. Application of MOFs and COFs for photocatalysis in CO_2 reduction, H_2 generation, and environmental treatment. *EnergyChem* **2022**, *4*, 100078−100121.

(12) Kuehn, S.; Sluyter, G.; Christlieb, M.; Heils, R.; Stoebener, A.; Kleber, J.; Smirnova, I.; Liese, A. In Situ Separation of the Chiral Target Compound (S)-2-Pentanol in Biocatalytic Reactive Distillation. *Ind. Eng. Chem. Res.* **2017**, *56*, 6451−6461.

(13) Bastida, A.; Sabuquillo, P.; Armisen, P.; Fernández-Lafuente, R.; Huguet, J.; Guisán, M. J. A single step purification, immobilization, and hyperactivation of lipases via interfacial adsorption on strongly hydrophobic supports. *Biotechnol. Bioeng.* **1998**, *58*, 486−493.

(14) Brady, C.; Metcalfe, L.; Slaboszewski, D.; Frank, D. Lipase immobilized on a hydrophobic, microporous support for the hydrolysis of fats. *J. Am. Oil Chem. Soc.* **1988**, *65*, 917−921.

(15) Manoel, E. A.; Dos Santos, J. C.; Freire, D. M. J.; Rueda, N.; Fernandez-Lafuente, R. Immobilization of lipases on hydrophobic supports involves the open form of the enzyme. *Enzyme Microb. Technol.* **2015**, *71*, 53−57.

(16) Lafuente, R. F.; Armisé, N. P.; Sabuquillo, P.; Fernández-Lorente, G.; Guisán, J. M. Immobilization of lipases by selective adsorption on hydrophobic supports. *Chem. Phys. Lipids* **1998**, *93*, 185−197.

(17) Simons, J. W.; Gotz, F.; Egmond, M. R.; Verheij, H. M. Biochemical properties of staphylococcal (phospho) lipases. *Chem. Phys. Lipids* **1998**, *93*, 27−37.

(18) Xie, J.-L.; Cong, F.-D. The Lid and Interfacial Activity of Lipases. *Chin. J. Biochem. Mol. Biol.* **2011**, *27*, 499−504.

(19) Cajal, Y.; Svendsen, A.; Bolos, J. D.; Patkar, S. A.; Alsina, M. A. Effect of the lipid interface on the catalytic activity and spectroscopic properties of a fungal lipase. *Biochimie* **2000**, *82*, 1053−1061.

(20) Asmat, S.; Husain, Q.; Azam, A. Lipase immobilization on facile synthesized polyaniline-coated silver-functionalized graphene oxide nanocomposites as novel biocatalysts: stability and activity insights. *RSC Adv.* **2017**, *7*, 5019−5029.

(21) Mathesh, M.; Luan, B.; Akanbi, T. O.; Weber, J. K.; Liu, J.-Q.; Barrow, C. J.; Zhou, R.-H.; Yang, W.-R. Opening lids: modulation of lipase immobilization by graphene oxides. *Catalysis* **2016**, *6*, 4760−4768.

(22) Zhang, G.; Ma, J.; Wang, J.; Li, Y.; Zhang, G.; Zhang, F.; Fan, X. Lipase immobilized on graphene oxide as reusable biocatalyst. *Ind. Eng. Chem. Res.* **2014**, *53*, 19878−19883.

(23) Xie, W.; Huang, M. Immobilization of Candida rugosa lipase onto graphene oxide Fe_3O_4 nanocomposite: characterization and application for biodiesel production. *Energy Convers. Manage.* **2018**, *159*, 42−53.

(24) Meng, Y.; Liu, T.-L.; Yu, S.-S.; Cheng, Y.; Lu, J.; Wang, H.-S. A lignin-based carbon aerogel enhanced by graphene oxide and application in oil/water separation. *Fuel* **2020**, *278*, 118376−118384.

(25) Qian, Y.; Ismail, I. M.; Stein, A. Ultralight, high-surface-area, multifunctional graphene-based aerogels from self-assembly of graphene oxide and resol. *Carbon* **2014**, *68*, 221−231.

(26) Andjelkovic, I.; Tran, D. N.; Kabiri, S.; Azari, S.; Markovic, M.; Losic, D. Graphene aerogels decorated with alpha-FeOOH nanoparticles for efficient adsorption of arsenic from contaminated waters. *ACS Appl. Mater. Interfaces* **2015**, *7*, 9758−9766.

(27) Zhao, Y.; Hu, C.; Hu, Y.; Cheng, H.; Shi, G.; Qu, L. A. Versatile, Ultralight, Nitrogen doped graphene framework. *Angew. Chem., Int. Ed.* **2012**, *51*, 11371−11375.

(28) Zhu, Y.; Romain, C.; Williams, C. K. Sustainable polymers from renewable resources. *Nature* **2016**, *540*, 354−362.

(29) Wang, J.-F.; Zhang, D.-H.; Chu, F.-X. Wood-Derived Functional Polymeric Materials. *Adv. Mater.* **2021**, *33*, No. 2001135.

(30) Wei, D.; Wu, C.-X.; Jiang, G.; Sheng, X.-X.; Xie, Y.-H. Lignin-assisted construction of well-defined 3D graphene aerogel/PEG form-stable phase change composites towards efficient solar thermal energy storage. *Sol. Energy Mater. Sol. Cells* **2021**, *224*, 111013−111021.

(31) Chen, H.; Liu, T.-L.; Meng, Y.; Cheng, Y.; Lu, J.; Wang, H.-S. Novel graphene oxide/aminated lignin aerogels for enhanced adsorption of malachite green in wastewater. *Colloids Surf., A* **2020**, *603*, 125281−125290.

(32) Zeng, Z.-H.; Wang, C.-X.; Zhang, Y.-F.; Wang, P.-Y.; Shahabadi, S. I. S.; Pei, Y.-M.; Chen, M.-J.; Lu, X.-H. Ultralight and Highly Elastic Graphene/Lignin-Derived Carbon Nanocomposite Aerogels with Ultrahigh Electromagnetic Interference Shielding Performance. *ACS Appl. Mater. Interfaces* **2018**, *10*, 8205−8213.

(33) Dai, C.-L.; Sun, W.; Xu, Z.-Z.; Liu, J.-W.; Chen, J.; Zhu, Z.-X.; Li, L.; Zeng, H.-B. Assembly of Ultralight Dual Network Graphene Aerogel with Applications for Selective Oil Absorption. *Langmuir* **2020**, *36*, 13698−13707.
(34) Marsden, S. R.; Mestrom, L.; McMillan, D. G. G.; Hanefeld, U. Thermodynamically and Kinetically Controlled Reactions in Biocatalysis − from Concepts to Perspectives. *ChemCatChem* **2020**, *12*, 426−437.
(35) Yue, Y.-Y.; Li, Y.-W.; Cheng, W.-L.; Han, G.-P.; Lu, T.; Huang, C.-B.; Wu, Q.-L.; Jiang, J.-C. High strength and ultralight lignin-mediated fire-resistant aerogel for repeated oil/water separation. *Carbon* **2022**, *193*, 285−297.
(36) Yu, D.-H.; Wang, Z.; Zhao, L.; Cheng, Y.-M.; Cao, S.-G. Resolution of 2-octanol by SBA-15 immobilized Pseudomon as sp. Lipase. *J. Mol. Catal. B: Enzym.* **2007**, *48*, 64−69.
(37) Turner, S.; Yan, W.; Long, H.; Nelson, A. J.; Baker, A.; Lee, J. R.; Carraro, C.; Worsley, M. A.; Maboudian, R.; Zettl, A. Boron doping and defect engineering of graphene aerogels for ultrasensitive NO_2 detection. *J. Phys. Chem. C* **2018**, *122*, 20358−20365.
(38) Sarada, L.; Desnuelle, P. Action de la lipase pancreatique sur les esters en emulsion. *Biochim. Biophys. Acta* **1958**, *30*, 513−521.
(39) Bayramolu, G.; Yilmaz, M.; Arica, M. Y. Immobilization of a thermostable α-amylase onto reactive membranes: kinetics characterization and application to continuous starch hydrolysis. *J. Food Biochem.* **2004**, *84*, 591−599.
(40) Nirprit, S. D.; Jagdeep, K. Immobilization, stability and esterification studies of a lipase from a Bacillus sp. *Biotechnol. Appl. Biochem.* **2002**, *36*, 7−12.
(41) Andrade, M. A. C.; Andrade, F. A. C.; Phillips, R. S. Temperature and DMSO increase the enantioselectivity of hydrolysis of methyl alkyl dimethylmalonates catalyzed by pig liver esterase. *Bioorg. Med. Chem. Lett.* **1991**, *1*, 373−376.
(42) Lowry, O. H.; Rosebrough, N. J.; Farr, A. L.; Randall, R. J. Protein measurement with the folin phenol reagent. *J. Biol. Inorg. Chem.* **1951**, *193*, 265−275.
(43) Ma, L.; Persson, M.; Adlercreutz, P. Water activity dependence of lipase catalysis in organic media explains successful transesterification reactions. *Enzyme Microb. Technol.* **2002**, *31*, 1024−1029.
(44) Itoh, T.; Hanefeld, U. Enzyme Catalysis in Organic Synthesis. *Green Chem.* **2017**, *19*, 331−332.
(45) Ye, P.; Xu, Z.-K.; Wu, J.; Innocent, C.; Seta, P. Nanofibrous poly (acrylonitrile-co-maleic acid) membranes functionalized with gelatin and chitosan for lipase immobilization. *Biomaterials* **2006**, *27*, 4169−4176.

https://doi.org/10.1021/acsomega.2c06908
ACS Omega 2023, 8, 2435−2444